

Theoretical Study of Azido–Tetrazole Isomerism: Effect of Solvent and Substituents and Mechanism of Isomerization

Elena Cubero,[†] Modesto Orozco,^{*,†} and Francisco J. Luque^{*,‡}

Contribution from the Departament de Bioquímica i Biologia Molecular, Facultat de Química, Universitat de Barcelona, Martí i Franquès 1, Barcelona 08028, Spain, and Departament de Físicoquímica, Facultat de Farmàcia, Universitat de Barcelona, Avda Diagonal s/n, Barcelona 08028, Spain

Received August 4, 1997

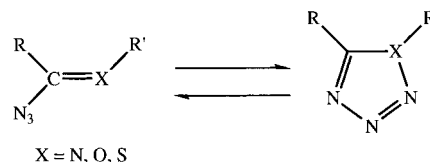
Abstract: We report the results of high-level ab initio calculations for the gas-phase interconversion of azido and tetrazole forms of thiazole[3,2-*d*]tetrazole. This study is supplemented with an analysis of the solvent effect on the isomerism using self-consistent reaction field (SCRf) and Monte Carlo-Free Energy Perturbation (MC-FEP) techniques in three different solvents: carbon tetrachloride, chloroform, and water. Finally, the influence exerted by the introduction of substituents on the relative population of isomers is also examined. The energy difference between azido and tetrazole species is found to be highly sensitive to the level of theory used to describe the gas-phase reaction. It also found that the free energies of solvation of azido and tetrazole species determined from SCRf or MC-FEP calculations allow us to predict the solvent-induced changes on the equilibrium. The results show that the azido form of thiazole[3,2-*d*]tetrazole is clearly disfavored as the solvent polarity increases. The influence played by substituents is also consistent with the experimental available data, it being shown that electron-withdrawing groups favor the azido isomer, while the opposite effect is observed for electron-donating substituents. The study demonstrates the capability of high-level quantum mechanical calculations combined with SCRf or MC-FEP results to analyze the azido–tetrazole isomerism and its dependence on the solvent and substituents.

Introduction

Despite the scarce presence of tetrazole in natural systems, the chemistry of this heterocycle has gained increasing attention since the early 1980s, mainly due to its role in a variety of synthetic and industrial processes.¹ This interest also stems from the ability of tetrazole to mimic the carboxylic acid group, which has motivated the incorporation of tetrazole in biologically active molecules.² Another research area of major interest is the therapeutic application of tetrazole, which has been included in pharmacologically active compounds with antihypertensive, antiallergic, and antibiotic activities.³

The reactivity of tetrazole is modulated by the deactivating effect of the three pyridine-type nitrogens, which overcome the influence of the single pyrrole-type nitrogen. As a result, the azapyrrole nucleus has a moderate stability, as reflected in a variety of chemical properties.^{1,4,5} Indeed, even though the

Scheme 1



integrity of the tetrazole ring is retained in reactions involving side groups, it is known that thermal degradation occurs both in the gas phase, mainly through N₂ elimination from the 2-NH tautomer, and in the melt, through formation of an acyclic azide. This latter process, i.e., the conversion of tetrazole to an acyclic azide, is likely the most clear evidence of the relative stability of this heterocycle.

The isomerism between cyclized and open species (Scheme 1), which is one of the main synthetic routes of tetrazoles,¹ is found in compounds of the general formula R–CXN₃–R',⁵ where R and R' are substituents on the adjacent carbon and heteroatom (X). The population of azido and tetrazole forms depends strongly on the nature of atom X.^{1,5a,6} In monocyclic

* To whom correspondence should be addressed.

[†] Facultat de Química.

[‡] Facultat de Farmàcia.

(1) Butler, R. N. In *Comprehensive Heterocyclic Chemistry*; Katritzky, A. R., Ress, C. W., Scriven, E. F. V., Eds.; Pergamon: Oxford, U.K., 1996; Vol. 4, p 621.

(2) (a) Zabrocki, J.; Smith, G. D.; Dunbar, J. B., Jr.; Iijima, H.; Marshall, G. R. *J. Am. Chem. Soc.* **1988**, *110*, 5875. (b) Yu, K. L.; Johnson, R. L. *J. Org. Chem.* **1987**, *52*, 2051. (c) Kojro, E.; Willhardt, I.; Rombach, A.; Grzonka, Z.; Hermann, P. *FEBS Lett.* **1987**, *212*, 83. (d) Kamiya, N.; Shiro, Y.; Iwata, T.; Iizuka, T.; Iwasaki, H. *J. Am. Chem. Soc.* **1991**, *113*, 1826. (e) Knotz, H.; Zbiral, E. *Liebigs Ann. Chem.* **1986**, 1736. (f) Hamed, A. *Synthesis* **1992**, 591. (g) Berner, S.; Muehlegger, K.; Seliger, H. *Nucleosides Nucleotides* **1988**, *7*, 763.

(3) (a) Singh, H.; Chawla, A. S.; Kapoor, V. K.; Paul, D.; Malhotra, R. K. In *Progress in Medicinal Chemistry*; Ellis, G. P., West, G. B., Eds.; Elsevier: North-Holland, 1980; Vol. 17, p 151. (b) Butler, R. N. *Adv. Heterocycl. Chem.* **1977**, *21*, 323.

(4) (a) McEwan, W. S.; Rigg, M. W. *J. Am. Chem. Soc.* **1951**, *73*, 4725. (b) Dewar, M. J. S.; Gleicher, G. J. *J. Chem. Phys.* **1966**, *44*, 759. (c) Markgraf, J. H.; Bachmann, W. T.; Hollis, D. P. *J. Org. Chem.* **1965**, *30*, 3472.

(5) (a) Elguero, J.; Claramunt, R. M.; Summers, A. J. H. *Adv. Heterocycl. Chem.* **1978**, *22*, 183. (b) Butler, R. N. *Chem. Ind.* **1973**, 371. (c) Tisler, M. *Synthesis* **1973**, *3*, 123. (d) Patai, S. In *The Chemistry of the Azido Group*; Wiley: New York, 1971. (e) Benson, F. R. In *Heterocyclic Compounds*; Elderfield, R. C., Ed.; Wiley: London, 1967; p 1 (f) Kauer, J. C.; Sheppard, W. A. *J. Org. Chem.* **1967**, *32*, 3580.

(6) (a) Lieber, E.; Minnis, R. L.; Rao, C. N. R. *Chem. Rev.* **1965**, *65*, 377. (b) Reynolds, G. A.; Van Allan, J. A.; Tinker, J. F. *J. Org. Chem.* **1959**, *24*, 1205.

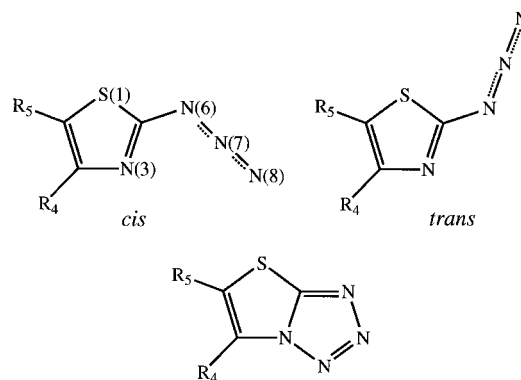
systems, the molecule is generally found in the acyclic form when X = O, and in the cyclic species, when X = S. When X = N, either form may predominate or both forms may exist in equilibrium. The isomerism is also modulated by the groups R and R' or by the aromatic nucleus to which the azido group is attached in heterocyclic compounds.^{5,7} As an empirical rule, electron-withdrawing substituents favor the azido form, while electron-donating groups enhance ring closure and stabilize the tetrazole form.^{8,9} The equilibrium also depends on the temperature.⁵ Cleavage of the tetrazole ring is generally an endothermic process,^{4a,5a,e,10} which explains that higher temperatures favor the azido species.^{7j,10d,11} Finally, the isomerism is determined by the state of the substance (solid or solution) and particularly by the solvent.⁵ In general, polar solvents favor the tetrazole form, and nonpolar solvents, the azido species.

Owing to the sensitivity to both solvent and substituents, the azido-tetrazole isomerism is an excellent chemical system to examine both the gas-phase and solvation contributions to the equilibrium. In the following, we report the results of the theoretical study of the isomerism of thiazole[3,2-*d*]tetrazole. This compound was chosen because the thiazole derivatives can be found in either the cyclized or open-chain forms under standard laboratory conditions, and the isomerism is particularly sensitive to substituent and solvent effects.^{5a,10d,12} Attention is paid to the factors controlling the gas-phase equilibrium, as well as the solvation influence in solvents of different polarity. In addition, the change in the equilibrium due to the presence of methyl or chlorine substituents in the thiazole ring is explored. Finally, the mechanism for the conversion between azido and tetrazole species is also studied.

Methods

Compounds. The isomerism reaction was studied considering the cyclized form and both *cis* and *trans* conformers of the azido species (Scheme 2). To investigate the mechanism for conversion between azido and tetrazole forms, the transition-state structure was also local-

Scheme 2



ized. Indeed, the effect of electron-donating and electron-withdrawing substituents was examined considering methyl and chloro derivatives in position 4 or 5 (see atom numbering in Scheme 2), which were chosen due to the availability of equilibrium constants in different solvents.^{12a,c}

Gas-Phase Calculations. Geometries were optimized at the HF level using the 6-31G(d), 6-311G(d), and 6-311++G(d,p) basis sets.¹³ The influence of electron correlation on geometrical parameters was examined from second-order Møller–Plesset¹⁴ calculations with the frozen-core approximation using the 6-31G(d) and 6-311G(d) basis sets. In all cases, the minimum energy or transition-state nature of the stationary points was verified from frequency analysis.

Single-point calculations at different levels of theory were performed using the MP2/6-311G(d)-optimized geometries to examine the convergence of results on basis set extension and higher-order electron correlation effects. Calculations at the HF and MP2 levels were carried out using the correlation-consistent valence double- (cc-pVDZ) and triple- ζ (cc-pVTZ) basis of Dunning,¹⁵ both with and without augmentation in the form of both diffuse functions (aug-cc-pVDZ) and functions of higher angular momentum (aug-cc-pVTZ), as well as with the 6-311++G(d,p) basis. These basis sets led respectively to 126, 272, 206, 418, and 202 contracted basis functions for thiazole[3,2-*d*]tetrazole. In addition, many-body perturbation theory up to fourth-order and quadratic single and double excitation with perturbative triple excitation¹⁶ were performed to examine the contribution of higher-order correlation effects. Owing to the cost of these latter calculations, they were carried out only with the 6-311++G(d,p) basis.

The thermodynamics in a vacuum was computed by correcting the differences in electronic energy to enthalpies at 298 K upon inclusion of zero-point energy and thermal corrections. The free energy differences were estimated from the addition of entropic corrections. All these terms were determined with the harmonic oscillator–rigid rotor¹⁷ approximation from the optimized geometries using the standard procedure in Gaussian-94.¹⁸

Finally, the electron density reorganization arising upon cyclization was analyzed using Bader's theory of atoms in molecules.¹⁹ Atomic

(7) (a) Benson, F. R.; Hartzel, L. W.; Otten, E. A. *J. Am. Chem. Soc.* **1954**, *76*, 1858. (b) Boyer, J. H.; Miller, E. J., Jr. *J. Am. Chem. Soc.* **1959**, *81*, 4671. (c) Boyer, J. H.; Hyde, H. W. *J. Org. Chem.* **1960**, *25*, 458. (d) Temple, C., Jr.; McKee, R. L.; Montgomery, J. A. *J. Org. Chem.* **1962**, *27*, 1671. (e) Temple, C., Jr.; Montgomery, J. A. *Ibid.* **1965**, *30*, 826. (f) Temple, C., Jr.; McKee, R. L.; Montgomery, J. A. *Ibid.* **1965**, *30*, 829. (g) Scott, F. L.; Cronin, D. A.; O'Halloran, J. K. *J. Chem. Soc. C* **1971**, 2769. (h) Alcalde, E.; de Medoza, J.; Elguero, J. *J. Chem. Soc., Chem. Commun.* **1974**, 411. (i) Elguero, J.; Fruchier, A.; Knutsson, L.; Lazaro, R.; Sandström, J. *Can. J. Chem.* **1974**, *52*, 2744. (j) Alcalde, E.; Claramunt, R. M. *Tetrahedron Lett.* **1975**, *18*, 1523. (k) Shishoo, C. J.; Jain, K. S. *J. Heterocycl. Chem.* **1992**, *29*, 883. (l) Steinschifter, W.; Stadlbauer, W. *J. Prakt. Chem.* **1994**, *336*, 311.

(8) (a) Butler, R. N.; Scott, F. L. *J. Org. Chem.* **1966**, *31*, 3182. (b) Norris, W. P.; Henry, R. A. *J. Org. Chem.* **1964**, *29*, 650. (c) Stanovnik, B.; Tisler, M. *Tetrahedron* **1969**, *25*, 3313. (d) Eloy, F. *J. Org. Chem.* **1961**, *26*, 952.

(9) (a) Lieber, E.; Sherman, E.; Henry, R. A.; Cohen, J. *J. Am. Chem. Soc.* **1951**, *73*, 2327. (b) Henry, R. A.; Finnegan, W. G.; Lieber, E. *J. Am. Chem. Soc.* **1955**, *77*, 2265.

(10) (a) Temple, C.; Thorpe, M. C.; Coburn, W. C.; Montgomery, J. A. *J. Org. Chem.* **1966**, *31*, 935. (b) C. Sasaki, T.; Kanematsu, K.; Murata, M. *Tetrahedron* **1971**, *27*, 5121. (c) Granados, R.; Rull, M.; Vilarrasa, J. *J. Heterocycl. Chem.* **1976**, *13*, 281. (d) Faure, R.; Galy, J. P.; Vincent, E. J.; Fayet, J. P.; Mauret, P.; Vertut, M. C.; Elguero, J. *Can. J. Chem.* **1977**, *55*, 1728.

(11) (a) Nguyen, M. T.; Leroy, G.; Sana, M.; Elguero, J. *J. Heterocycl. Chem.* **1982**, *19*, 943. (b) L'abbé, G. *J. Heterocycl. Chem.* **1984**, *21*, 627.

(12) (a) Elguero, J.; Faure, R.; Galy, J. P.; Vincent, E. *J. Anal. Quim.* **1980**, *76*, 211. (b) Hanoun, J. P.; Faure, R.; Galy, J. P.; Elguero, J. *J. Heterocycl. Chem.* **1996**, *33*, 747. (c) Elguero, J.; Faure, R.; Galy, J. P.; Vincent, E. *Bull. Soc. Chim. Belg.* **1975**, *84*, 1189. (d) Faure, R.; Galy, J. P.; Giusti, G.; Vincent, E. J.; Elguero, J. *Org. Magn. Res.* **1974**, *6*, 485. (e) Faure, R.; Galy, J. P.; Vincent, E. J.; Elguero, J. *J. Heterocycl. Chem.* **1977**, *14*, 1299.

(13) (a) Hariharan, P. C.; Pople, J. A. *Theor. Chim. Acta* **1973**, *28*, 213. (b) McLean, A. D.; Chandler, G. S. *J. Chem. Phys.* **1980**, *72*, 5639. (c) Frisch, M. J.; Pople, J. A.; Binkley, J. S. *J. Chem. Phys.* **1984**, *80*, 3265.

(14) Møller, C.; Plesset, M. S. *Phys. Rev.* **1934**, *46*, 618.

(15) Dunning, T. H., Jr. *J. Chem. Phys.* **1989**, *90*, 1007.

(16) (a) Pople, J. A.; Head-Gordon, M.; Raghavachari, K. *J. Chem. Phys.* **1987**, *87*, 5968. (b) Gauss, J.; Cremer, C. *Chem. Phys. Lett.* **1988**, *150*, 280. (c) Slater, E. A.; Trucks, G. W.; Bartlett, R. J. *J. Chem. Phys.* **1989**, *90*, 1752.

(17) McQuerrrie, D. *Statistical Mechanics*; Harper & Brown: New York, 1976.

(18) Frisch, M. J.; Trucks, G. W.; Schlegel, H. B.; Gill, P. M. W.; Johnson, B. G.; Robb, M. A.; Cheeseman, J. R.; Keith, T. A.; Petersson, G. A.; Montgomery, J. A.; Raghavachari, K.; Al-Laham, M. A.; Zakrzewski, V. G.; Ortiz, J. V.; Foresman, J. B.; Cioslowski, J.; Stefanov, B. B.; Nanayakkara, A.; Challacombe, M.; Peng, C. Y.; Ayala, P. Y.; Chen, W.; Wong, M. W.; Andres, J. L.; Replogle, E. S.; Gomperts, R.; Martin, R. L.; Fox, D. J.; Binkley, J. S.; Defress, D. J.; Baker, J.; Stewart, J. J. P.; Head-Gordon, M.; Gonzalez, C.; Pople, J. A. *GAUSSIAN 94* (Rev. A.1), GAUSSIAN Inc.: Pittsburgh, PA, 1995.

charges were determined by integration of the electron density in regions enclosed within the zero-flux surfaces. Moreover, the location of the (3, -1) bond critical points, which can be related to the formation of chemical bond,²⁰ was determined and the electron density was computed at the critical points to obtain a measure of the bond order.²¹ Finally, molecular electrostatic potentials (MEP)²² were computed to examine the changes in chemical reactivity due to the charge density redistribution. All of these analyses were performed at the MP2/6-311G(d) level.

Calculations in Solution. To examine the solvent effect on the isomerism, the free energies of solvation were determined using self-consistent reaction field (SCRf) and Monte Carlo free energy perturbation (MC-FEP) calculations. Three different solvents (carbon tetrachloride, chloroform, and water) were considered to explore the influence of increasing the dielectric permittivity on the relative population between isomers.

SCRf calculations were performed using the MST model,²³ also known as polarizable continuum model.²⁴ Computations were carried out with our optimized ab initio HF/6-31G(d) version of the MST method,^{23c,25} which was parametrized for carbon tetrachloride, chloroform, and water. The gas-phase MP2/6-311G(d)-optimized geometry was used in calculations. The effect of geometry relaxation in solution on the relative free energies of solvation was also examined by using the geometry optimization algorithm recently developed in the framework of the same method by the Pisa group.^{26,27}

MC-FEP simulations²⁸ were performed using the windowing scheme, with 21 double-wide sampling windows. The transition state was mutated to the tetrazole and *cis*-azido isomers. This latter species was also mutated to the *trans*-azido form to explore the solvent effect on the conformational equilibrium of azido species. Each window consisted of 2 million configurations for equilibration and 3 million configurations for averaging. The hysteresis was computed as half the difference between forward and reverse paths, and the standard deviation in the free energy of solvation was determined from six partial averages of 0.5 million configurations in each window. The simulation system consisted of the solute embedded in 120, 126, and 500 solvent molecules for calculations in carbon tetrachloride, chloroform, and water. Simulations were performed at the isothermic-isobaric ensemble (NPT; 1 atm, 298 K) using periodic boundary conditions with a 10 Å cutoff for solute-solvent interactions and 9 Å cutoff for solvent-solvent interactions. The geometry of the solute was mutated along the simulation, but no sampling of the internal degrees of freedom was performed. Parameters determining volume changes and solute rotations and translations were adjusted to have an acceptance level around 40%. Atomic charges for the solute were determined by fitting the electrostatic potential computed at the MP2/6-311G(d) level using the standard

procedure.²⁹ The van der Waals parameters were taken from the OPLS force field. The standard OPLS parameters for carbon tetrachloride, chloroform, and TIP4P water molecules were used.³⁰

Finally, the MEPs²² for the species in solution were determined from the wave function of the solute fully polarized by the solvent. This allowed us to examine the changes in the charge density distribution originated upon solvation.

Computational Packages. Calculations in the gas phase were carried out with Gaussian-94.¹⁸ MST calculations were performed with a modified version of MonsterGauss.³¹ Geometry optimizations in solution were performed with HONDO-8,³² which was modified by the Pisa group to include the optimization algorithm in SCRf calculations. Monte Carlo simulations were done using BOSS 3.4.³³ Bond critical points were determined with the program AIMPAC.³⁷ MEPs were computed using MOPETE/MOPFIT.³⁴ Calculations were performed on the IBM-SP2 computer of the Centre de Supercomputació de Catalunya and SGI and HP workstations.

Results and Discussion

Molecular Geometries. Owing to the electron density redistribution arising upon cyclization, we examined the influence of basis set and electron correlation on the geometries. The structural parameters were optimized at the HF and MP2 levels using bases ranging from 6-31G(d) to 6-311++G(d,p). Analysis of the optimized geometries (available as Supporting Information) showed that extension of the basis had negligible influence. However, inclusion of electron correlation led to very relevant changes for some bond lengths (up to 0.08 Å with regard to the HF values) in both azido and tetrazole moieties, as well as in the thiazole ring, indicating that treatment of electron correlation is needed to describe the geometrical parameters. The MP2/6-311G(d)-optimized bond lengths and angles are given in Table 1, which also reports the values for the crystal structures of 4-phenyl-3(5)azidopyrazole and tetrazole[1,5-*b*]benzothiazole.³⁶ Even though comparison with X-ray data must be performed with caution owing to the different nature of the aromatic core, it is clear that the optimized parameters agree well with the X-ray values, which suggests that geometry optimization at higher-order electron correlation levels has little influence on the structural parameters.

The results in Table 1 show that, in addition to the loss of linearity of the azido group, which bends around 60°, the most relevant changes upon cyclization concern the angles N3-C2-N6 and C2-N6-N7, which vary 10–17°, the bonds N6-N7

(19) (a) Bader, R. F. W. *Atoms in Molecules. A Quantum Theory*; Clarendon: Oxford, U.K., 1990. (b) Bader, R. F. W. *Chem. Rev.* **1991**, *91*, 893. (c) Bader, R. F. W.; Carroll, M. T.; Cheeseman, J. R.; Chang, C. J. *Am. Chem. Soc.* **1987**, *109*, 7968.

(20) (a) Boyd, R. J.; Wang, L.-C. *J. Comput. Chem.* **1989**, *10*, 367. (b) Cioslowski, J.; Mixon, S. T. *J. Am. Chem. Soc.* **1992**, *114*, 4382. (c) Bader, R. F. W.; Essen, H. J. *Chem. Phys.* **1984**, *80*, 1943.

(21) (a) Bader, R. F. W.; Slee, T. S.; Cremer, D.; Kraka, E. *J. Am. Chem. Soc.* **1983**, *105*, 5061. (b) Boyd, R. J. *Stud. Org. Chem.* **1987**, *31*, 485. (c) Wiber, K. B.; Bader, R. F. W.; Lau, C. D. H. *J. Am. Chem. Soc.* **1987**, *109*, 985.

(22) Scrocco, E.; Tomasi, J. *Top. Curr. Chem.* **1973**, *42*, 95.

(23) (a) Luque, F. J.; Bachs, M.; Orozco, M. *J. Comput. Chem.* **1994**, *15*, 847. (b) Orozco, M.; Bachs, M.; Luque, F. J. *J. Comput. Chem.* **1995**, *16*, 563. (c) Bachs, M.; Luque, F. J.; Orozco, M. *J. Comput. Chem.* **1994**, *15*, 446.

(24) (a) Miertus, S.; Scrocco, E.; Tomasi, J. *Chem. Phys.* **1981**, *55*, 117. (b) Miertus, S.; Tomasi, J. *Chem. Phys.* **1982**, *65*, 239. (c) Tomasi, J.; Persico, M. *Chem. Rev.* **1994**, *94*, 2027.

(25) (a) Luque, F. J.; Bachs, M.; Aleman, C.; Orozco, M. *J. Comput. Chem.* **1996**, *17*, 806. (b) Luque, F. J.; Zhang, Y.; Aleman, C.; Bachs, M.; Gao, J.; Orozco, M. *J. Phys. Chem.* **1996**, *100*, 4269.

(26) (a) Cammi, M.; Tomasi, J. *J. Chem. Phys.* **1994**, *101*, 7495. (b) *Ibid.* **1994**, *101*, 3888. (c) Cossi, M.; Mennucci, B.; Cammi, R. *J. Comput. Chem.* **1996**, *17*, 57.

(27) Cossi, M.; Tomasi, J.; Cammi, R. *Int. J. Quantum Chem. Symp.* **1995**, *29*, 695.

(28) Zwanzig, R. W. *J. Chem. Phys.* **1954**, *22*, 1420.

(29) (a) Momany, F. A. *J. Phys. Chem.* **1978**, *82*, 592. (b) Singh, U. C.; Kollman, P. A. *J. Comput. Chem.* **1984**, *5*, 129. (c) Orozco, M.; Luque, F. J. *J. Comput.-Aided Mol. Des.* **1990**, *4*, 411.

(30) (a) Jorgensen, W. L.; Chandrasekhar, J.; Madura, J. D.; Impey, R.; Klein, M. *J. Chem. Phys.* **1983**, *79*, 296. (b) Jorgensen, W. L.; Briggs, J. M.; Contreras, M. L. *J. Phys. Chem.* **1990**, *94*, 1683.

(31) Peterson, M.; Poirier, R. *MonsterGauss*; Department of Chemistry, University of Toronto: Toronto, Canada. Modified by R. Cammi, R. Bonaccorsi, and J. Tomasi, University of Pisa, Italy, 1987. Modified by F. J. Luque and M. Orozco, University of Barcelona, Spain, 1995.

(32) Dupuis, M.; Farazdel, A.; Karma, S. A.; Maluendes, S. A. *HONDO-8*; IBM-corporation Scientific and Engineering Computations: Kinross, NY. Modified by M. Cossi, R. Cammi, and J. Tomasi, University of Pisa, Italy, 1994.

(33) Jorgensen, W. L. *BOSS*, version 3.4; Yale University: New Haven, CT, 1990.

(34) Biegler-König, F.; Bader, R. F. W.; Tang, T.-H. *J. Comput. Chem.* **1982**, *3*, 317.

(35) Luque, F. J.; Orozco, M. Unpublished version of MOPETE/MOPFIT computer program, University of Barcelona, Spain.

(36) (a) Domiano, P.; Musatti, A. *Cryst. Struct. Commun.* **1974**, *3*, 713. (b) *Ibid.* **1974**, *3*, 335.

(37) (a) Szabo, A.; Ostlund, N. S. *Modern Quantum Chemistry*; MacMillan: New York, 1982. (b) Nobes, R. H.; Pople, J. A.; Radom, L.; Handy, N. C.; Knowles, P. J. *Chem. Phys. Lett.* **1987**, *138*, 481. (c) Falvey, D. E.; Cramer, C. J. *Tetrahedron Lett.* **1992**, *33*, 1705. (d) Cramer, C. J.; Truhlar, D. G. *J. Am. Chem. Soc.* **1993**, *115*, 8810.

Table 1. Structural Parameters Optimized at the MP2/611G(d) Level for the Azido and Tetrazole Forms

bond lengths (Å)	S1–C2	S1–C5	C2–N3	N3–C4	C4–C5	C2–N6	N6–N7	N7–N8	N3–N8
<i>cis</i> -azido	1.727	1.719	1.312	1.374	1.374	1.402	1.245	1.152	—
exptl ^a			1.361			1.407	1.244	1.140	
<i>trans</i> -azido	1.746	1.717	1.309	1.370	1.375	1.402	1.240	1.155	—
tetrazole	1.725	1.746	1.362	1.388	1.361	1.328	1.356	1.331	1.342
exptl ^b	1.728	1.771	1.344	1.403	1.389	1.322	1.372	1.309	1.352
bond angles (deg)	C5–S1–C2	S1–C2–N3	S1–C5–C4	C2–N3–C4	N3–C4–C5	N3–C2–N6	C2–N6–N7	N6–N7–N8	N7–N8–N3
<i>cis</i> -azido	88.4	116.5	110.2	109.1	115.9	125.7	114.1	172.5	—
exptl ^a						121.5	114.2	171.9	
<i>trans</i> -azido	88.4	115.8	110.1	109.5	116.2	120.3	117.6	172.0	—
tetrazole	89.3	111.2	114.0	115.7	109.8	109.0	104.7	112.6	104.6
exptl ^b	89.0	112.5	113.3	116.3	109.0	109.3	104.2	112.6	104.5

^a Reference 36a. ^b Reference 36b.

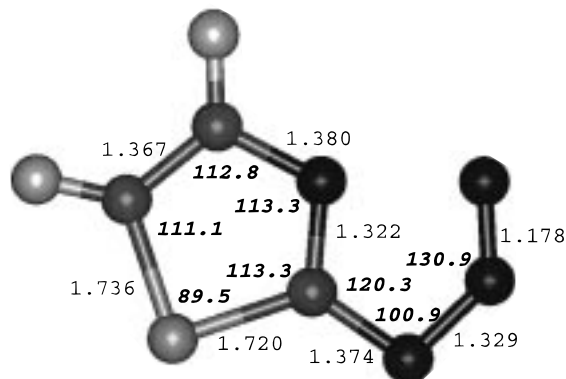


Figure 1. Structural parameters of the transition-state structure. The geometry was optimized at the MP2/6-311G(d) level. Bond lengths are given in angstroms.

and N7–N8, which increase 0.11 and 0.18 Å, and the bond C2–N6, which decreases 0.07 Å. The changes in the thiazole ring are less important and involve mainly atoms C2 and N3: the bond C2–N3 increases 0.05 Å, and the angles S1–C2–N3, C2–N3–C4, and N3–C4–C5 vary around 6°. These changes reveal the magnitude of the electron density redistribution, which will be examined in detail below. As expected, the optimized parameters for the transition state (TS; Figure 1) are intermediate between those of azido and tetrazole. However, the change in structural parameters along the cyclization is highly asynchronous. Thus, the bonds N7–N8, C2–N3, and N6–N7 at the TS are enlarged 0.03, 0.01, and 0.08 Å with regard to their values in the *cis*-azido, while they differ 0.18, 0.05, and 0.11 Å between *cis*-azido and tetrazole. A similar finding is observed for the bond angles, as noted in the distortion of the azido group (~40°) upon conversion from the *cis*-azido to the TS, but also in the changes of angles N3–C2–N6 and C2–N6–N7.

The preceding analysis indicates that different events occur as the azido group cyclizes, which agrees with the proposal of Burke et al.³⁸ The conversion *cis*-azido → TS involves basically bending of the angle N6–N7–N8 with increase in the length of N6–N7 and decrease in the length of C2–N6, while the bond N7–N8 remains little affected. The ring cyclization occurs mainly in the conversion TS → tetrazole, in which the bond length N3–N8 varies from 1.91 to 1.34 Å with concomitant changes in the bonds N7–N8 and C2–N3, which are enlarged 0.15 and 0.04 Å, and the angle N3–C2–N6, which decreases around 11°.

Gas-Phase Thermodynamics. Table 2 shows the relative gas-phase energies obtained at the various calculational levels

Table 2. Relative Gas-Phase Energies, Enthalpies, and Free Energy Differences (kcal/mol) of *trans*-Azido, Tetrazole, and Transition-State (TS) Species^a

method	<i>trans</i> -azido	tetrazole	TS
HF/6-31G(d)	5.2	0.3	26.8
HF/6-311G(d)	5.4	1.7	27.6
HF/6-311++G(d,p)	5.6	1.5	27.9
HF/cc-pVDZ	5.0	1.6	27.0
HF/aug-cc-pVDZ	4.5	-0.1	27.1
HF/cc-pVTZ	4.8	2.0	28.2
HF/aug-cc-pVTZ	4.5	1.9	28.2
MP2/6-31G(d)	2.4	4.4	29.0
MP2/6-311G(d)	2.7	7.2	30.8
MP2/6-311++G(d,p)	3.3	7.1	30.8
MP2/cc-pVDZ	2.3	6.6	29.8
MP2/aug-cc-pVDZ	2.0	3.3	27.8
MP2/cc-pVTZ	2.3	5.2	29.2
MP2/aug-cc-pVTZ	2.2	4.3	28.7
MP3/6-311++G(d,p)	4.7	-2.1	26.0
MP4(DQ)/6-311++G(d,p)	4.8	2.2	28.9
MP4(SDQ)/6-311++G(d,p)	4.3	5.1	26.5
MP4(SDTQ)/6-311++G(d,p)	3.0	7.8	25.0
QCISD/6-311++G(d,p)	4.3	3.7	24.5
QCISD(T)/6-311++G(d,p)	3.7	4.0	22.5
best estimate ^b	2.6	1.2	20.4
ZPE ^c	-0.1	1.1	-0.3
$\Delta E^{\ddagger d}$	0.0	-0.7	-0.7
ΔH	2.5	1.6	19.4
$-T\Delta S^{\ddagger d}$	-0.2	1.9	1.7
ΔG	2.3	3.5	21.1

^a All values are given relative to the *cis*-azido isomer. The MP2/6-311G(d)-optimized geometry was used in calculations. ^b See text for explanations. ^c Zero-point energy. ^d Thermal (ΔE^{\ddagger}) and entropy ($-T\Delta S^{\ddagger}$) corrections determined at 298 K.

using the MP2/6-311G(d)-optimized geometries. The energy differences are reasonably converged at both HF and MP2 levels for the different chemical species. The results derived from calculations performed with the cc-pVDZ and cc-pVTZ basis sets are generally close to the energy differences determined with the 6-311G(d) basis. Augmentation of Dunning's basis sets influences exclusively the relative energy of tetrazole, this effect being less pronounced for the cc-pVTZ basis.

Comparison of HF and MP2 results shows the large influence of electron correlation on the relative energies. To examine the contribution of higher-order electron correlation effects, Møller–Plesset calculations up to fourth-order were performed using the 6-311++G(d,p) basis. The results (Table 2) show that higher-order terms greatly influences the relative stability of tetrazole. Thus, despite the similarity of energy differences computed at the MP4(SDTQ) and MP2 levels, the MP_x values do not show a clear convergence, as expected from previous studies of conjugated π systems.³⁷ Accordingly, we performed QCISD and QCISD(T) calculations, which showed that the

(38) Burke, L. A.; Elguero, J.; Leroy, G.; Sana, M. *J. Am. Chem. Soc.* 1976, 98, 1685.

Table 3. Net Atomic Populations and Electron Density at the (3, -1) Bond Critical Points of *cis*-Azido, Tetrazole, and Transition-State (TS) Species Determined at the MP2/6-311G(d) Level^a

	Net Charge								
	S1	C2	N3	C4	C5	N6	N7	N8	
<i>cis</i> -azido	0.31	0.83	-1.10	0.42	-0.28	-0.47	-0.06	0.13	
TS	0.36	0.73	-1.03	0.39	-0.24	-0.48	-0.05	0.05	
tetrazole	0.36	0.71	-0.84	0.42	-0.21	-0.57	-0.05	-0.07	
	Bond Critical Points								
	S1–C2	S1–C5	C2–N3	N3–C4	C4–C5	C2–N6	N6–N7	N7–N8	N3–N8
<i>cis</i> -azido	0.211	0.212	0.358	0.309	0.313	0.286	0.429	0.538	—
TS	0.211	0.207	0.344	0.295	0.317	0.320	0.366	0.540	0.094
tetrazole	0.209	0.202	0.314	0.284	0.321	0.354	0.363	0.390	0.368

^a All properties in atomic units.

relative energy for the *trans*-azido is reasonably converged, while higher-order single and double excitations have a stabilizing effect for the tetrazole.

The preceding results emphasize the sensitivity to higher-order electron correlation effects, which stems from the large changes of electron density in the azido–tetrazole isomerism. It seems then reasonable to use as our best estimate of the relative energy between isomers the difference between QCISD-(T) and MP2 results computed with the 6-311++G(d,p) basis and to add these differences to the values calculated at the MP2 level with the aug-cc-pVTZ basis. The final values (Table 2) indicate that *trans*-azido and tetrazole are destabilized 2.6 and 1.2 kcal/mol with regard to the *cis*-azido. Our results clearly differ from the values reported in previous studies on the gas-phase isomerism of 1*H*-tetrazole, where the tetrazole was more stable by 66 kcal/mol at the HF/STO-3G level,³⁸ and imidazo-[1,2-*d*]tetrazole, where the tetrazole was also preferred by near 9 kcal/mol at the semiempirical MNDO level.³⁹

The zero-point energy and thermal and entropic corrections determined from the MP2/6-311G(d)-optimized geometries are given in Table 2. The contribution of these terms to the free energy difference between *cis*- and *trans*-azido forms is negligible. However, they make a significant contribution to the relative stability of tetrazole, which is destabilized by 2.3 kcal/mol, this effect being mainly due to the loss of degrees of freedom upon cyclization. The differences in free energy with regard to the *cis*-azido form are 2.3 and 3.5 kcal/mol for *trans*-azido and tetrazole, respectively, which indicate that the population of the tetrazole form is estimated to be less than 0.3%. This finding agrees with the experimentally predicted gas-phase preference of the azido species over the tetrazole form by around 4 kcal/mol for thiazole[3,2-*d*]tetrazole.^{12c}

Table 2 also gives the energy difference of the TS relative to the *cis*-azido isomer. As noted before, the relative energy is well-converged upon basis set extension at both HF and MP2 levels. However, higher-order electron correlation terms reduces sensibly the energy difference. Following the procedure mentioned above, the relative energy is found to be 20.4 kcal/mol, which differs substantially from the values reported in previous theoretical studies.^{38,39} Inclusion of zero-point energy and thermal and entropy corrections allows to estimate the gas-phase free energy difference to be 21.1 and 17.6 kcal/mol relative to *cis*-azido and tetrazole isomers.

Mechanism of Cyclization. To gain insight into the electron density redistribution in the cyclization, we examined the changes in Bader's atomic charges and in the electron density at the bond critical points (Table 3). Inspection of the charges indicates that most of the electron density redistribution occurs

in the conversion TS → tetrazole, where the charges of N3, N6, and N8 vary 0.1–0.2 *e*. On the contrary, the conversion *cis*-azido → TS affects preferentially atoms C2, N3, and N8, whose partial charge varies by less than 0.1 *e*.

The largest changes in electron density at the bond critical points for the conversion *cis*-azido → TS occur at bonds C2–N6 and N6–N7, where the electron density increases by 0.034 and decreases by 0.063 (in atomic units), respectively. There is also a loss of electron density (around 0.014) at C2–N3 and N3–C4. These changes agree with the enlargement of N6–N7 (0.08 Å), C2–N3 (0.01 Å), and N3–C4 (0.01 Å) and the shortening of C2–N6 (0.03 Å). It is worth noting that the initial formation of the bond between N3 and N8 is reflected in the appearance of the critical point between the two atoms, whereas the electron density at the critical point of N7–N8 remains nearly unchanged. Regarding the conversion TS → tetrazole, the most relevant changes occur at the critical points of N3–N8, where the bond formation is reflected in the increase of electron density by 0.274, and of N7–N8, where the electron density decreases by 0.150. These variations agree with the shortening of N3–N8 by near 0.6 Å and the enlargement of the N7–N8 by 0.15 Å. The changes at C2–N6 and C2–N3 are also remarkable. On the contrary, the electron density at the critical point of N6–N7 is very little affected.

The preceding data provide a detailed picture of the changes in electron density in the reaction. Bending of the azido group through the angle N6–N7–N8 promotes an electron transfer from the bond N6–N7 to C2–N6, concomitant with the incipient attack of the lone pair on N3 to the bond N7–N8. This is reflected in the decrease of positive charge of C2 and in the charge transfer from N3 to N8. Indeed, the lone pair on N6 is enhanced, in agreement with the reduction of the angle C2–N6–N7 from 114.1 (*cis*-azido) to 100.9 (TS) degrees, as it is also shown in the MEP maps for these structures (Figure 2). Thus, the MEP minimum on N6 varies from -23.7 (*cis*-azido) to -50.4 (TS) kcal/mol, this change being notably larger than the variation in the MEP minimum on N8, which varies from -17.6 (*cis*-azido) to -25.2 (TS) kcal/mol.

The ring cyclization is accompanied by an electron shift from N3 to N8 in conjunction with the formation of the lone pair on N7 from the electron density between atoms N7 and N8, whose sp² character is enhanced, as reflected in the change of their structural parameters, but also in the MEP maps for TS and tetrazole (Figure 2). Thus, the MEP minimum on N7, which is absent in the TS, amounts to -60.9 kcal/mol in the tetrazole, and the MEP minimum around N8 in the tetrazole is 18 kcal/mol larger than the value in the TS. Nevertheless, there are little changes in the MEP around N6. This means that the charge variation on N6 reflects the enhanced double bond between C2 and N6, as noted in the increase of electron density

(39) Olivella, S.; Vilarrasa, J.J. *Heterocycl. Chem.* **1979**, *16*, 685.

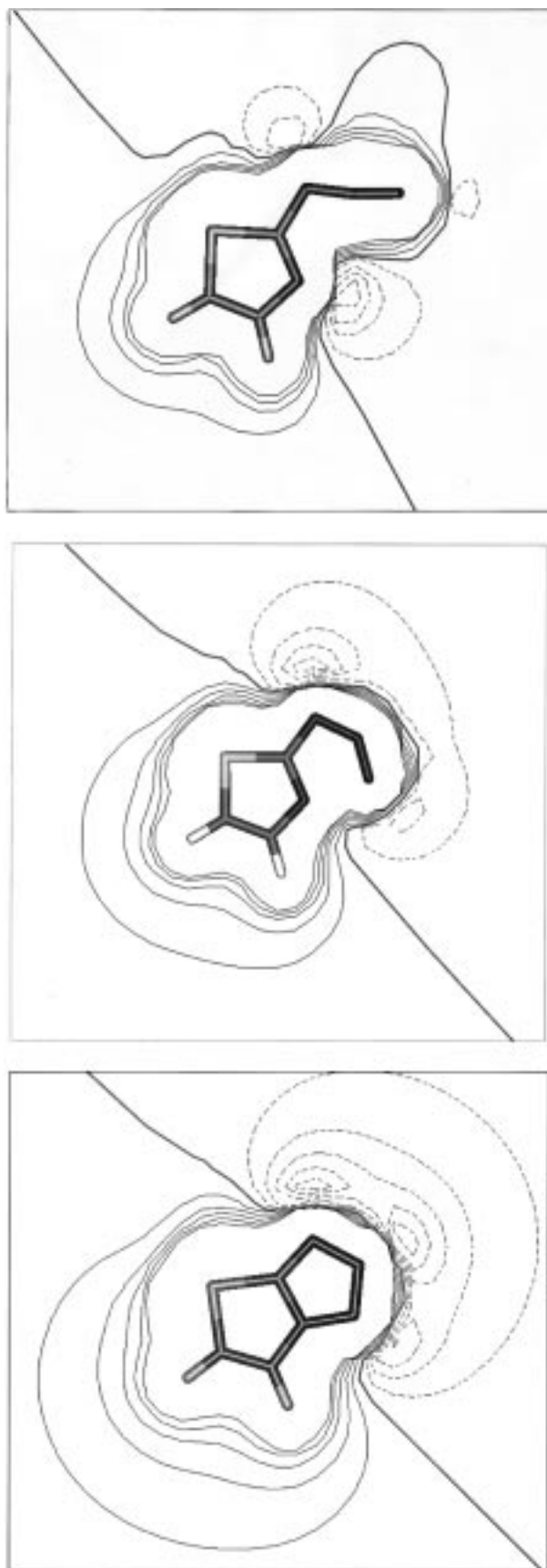


Figure 2. Electrostatic potential distribution in the gas phase for the *cis*-azido (A, top), transition state (B, center), and tetrazole (C, bottom). The isocontour lines are 0, $\pm 10.$, $\pm 20.$, $\pm 30.$, $\pm 40.$, and $\pm 50.$ kcal/mol for the transition state and tetrazole and 0, $\pm 10.$, $\pm 20.$, $\pm 30.$, and $\pm 40.$ kcal/mol for *cis*-azido. Negative values are in dashed lines. The zero isocontour line is in bold.

Table 4. Relative Free Energies of Solvation (kcal/mol) of *trans*-Azido, Tetrazole, and Transition-State (TS) Species in Carbon Tetrachloride, Chloroform, and Aqueous Solution Determined from SCRf MST and MC-FEP ^aCalculations^b

method	<i>trans</i> -azido	tetrazole	TS
Carbon Tetrachloride			
MST	-0.1	-1.0	0.0
MC-FEP	0.1	-0.7	-0.4
Chloroform			
MST	-0.5	-2.3	-0.2
MC-FEP	-0.4	-2.4	-0.8
Aqueous Solution			
MST	-2.4	-6.8	-1.0
MC-FEP	-1.6	-6.2	-1.5

^a The profiles for the mutations in MC-FEP simulations were smooth and no discontinuity was observed. The hysteresis was lower than 0.1 kcal/mol and the standard deviation was smaller than 0.2 kcal/mol. ^b Values are given relative to the free energy of solvation of the *cis*-azido isomer. The MP2/6-311G(d) gas-phase optimized geometry was used in calculations.

at the bond critical point, which compares with the decrease of electron density between C2 and N3.

Free Energies of Solvation. SCRf-MST and MC-FEP calculations were performed to determine the relative free energies of solvation (Table 4). In general, there is close agreement between the MST and MC-FEP results for the three solvents. The largest discrepancy is found for the relative free energy of solvation between *cis*- and *trans*-azido in water. Overall, considering the methodological differences of the two techniques, the similarity between MST and MC-FEP values gives confidence in the results.

The effect of solvent-induced geometry relaxation on the relative free energy of solvation was examined only in water, since very modest changes in geometry are expected in apolar solvents.⁴⁰ The geometry of azido and tetrazole isomers was fully optimized in aqueous solution using the MST HF/6-31G(d) direct algorithm.²⁶ It was found that water induces very small changes on the structural parameters, which are much lower than the differences found between HF and MP2-optimized geometries in the gas phase, and the effect of these geometrical changes on the relative free energy of solvation is negligible. Similar trends were also found upon relaxation of the TS geometry. These findings support the use of gas-phase-optimized geometries in MST and MC-FEP calculations.

The great influence of the solvent on the relative stabilities is clear from the values in Table 4. Both *trans*-azido and tetrazole, and to a lesser extent the TS, are stabilized better than *cis*-azido upon solvation, this effect being larger as the polarity of the solvent increases. In fact, in water, the tetrazole is better solvated than the *cis*-azido by 6–7 kcal/mol, which results from the difference in polarity of the two isomers (the gas-phase dipole moments are 2.4 (*cis*-azido) and 6.3 (tetrazole) D at the MP2/6-311G(d) level), and from the larger solvent-induced polarization of tetrazole, as noted in the difference maps for the MEP computed in the gas phase and in water (Figure 3). The enhanced polarity of tetrazole upon solvation is reflected in the larger variation of the electrostatic potential, this effect being sensibly lower in the case of the *cis*-azido isomer.

Thermodynamics in Solution. Table 5 reports the free energy differences in solution, which are determined from addition of the relative free energies of solvation to the gas-phase free energy differences. The tetrazole is found to be the

(40) (a) Luque, F. J.; Lopez-Bes, J. M.; Cemeli, J.; Aroztegui, M.; Orozco, M. *Theor. Chem. Acta* **1997**, *96*, 105. (b) Luque, F. J.; Cossi, M.; Tomasi, J. *Mol. Struct. (THEOCHEM)* **1996**, *371*, 123.

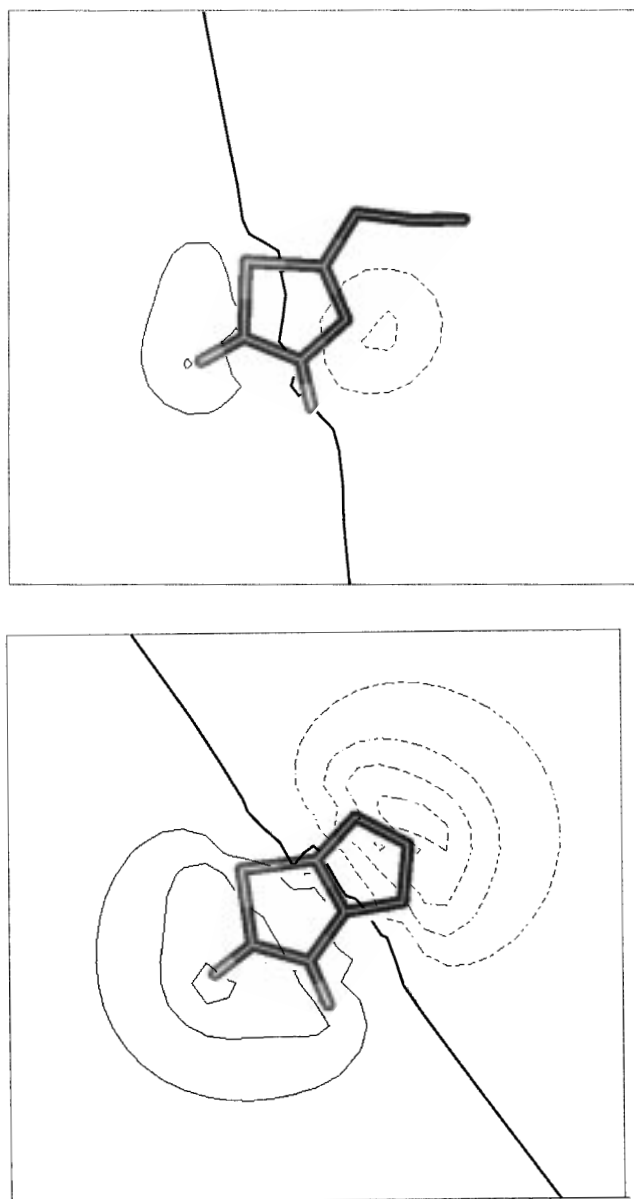


Figure 3. Difference maps between electrostatic potential distributions in the gas phase and in aqueous solution of the *cis*-azido (A, top) and tetrazole (B, bottom). The isocontour lines are $-10.$, $-5.$, $0.$, and $5.$ kcal/mol for *cis*-azido and $-20.$, $-15.$, $-10.$, $-5.$, $0.$, $5.$, $10.$, and $15.$ kcal/mol for tetrazole. Negative values are in dashed lines. The zero isocontour line is in bold.

most stable species in water, reverting the preference of the *cis*-azido in the gas phase. Comparison of the calculated and experimental equilibrium constants shows reasonable agreement. At this point, let us note that the experimental value in water is not available and the equilibrium constant collected in Table 5 corresponds to the most polar solvent (hexametapol).⁴¹

The stability of the TS increases with the polarity of the solvent. Nevertheless, this effect is rather small (~ 1 kcal/mol in water) and the free energy barrier is not drastically changed upon solvation, which suggests little variations in the kinetics upon solvation. However, our results do not allow us to exclude a more active participation of solvent molecules in controlling

(41) This is the most polar solvent for which the experimental equilibrium constant for the parent compound is available. In the case of methyl and chloro derivatives, the value in dimethyl sulfoxide was taken for comparison with the theoretical estimates in water.

Table 5. Free Energy Differences (kcal/mol) in Solution of *trans*-Azido, Tetrazole, and Transition-State (TS) Species with Regard to the *cis*-Azido Isomer^a and Equilibrium Constants for the Azidoazomethine-Tetrazole Isomerization

method	<i>trans</i> -azido	tetrazole	TS	$\log_{10} K$ (calcd) ^b	$\log_{10} K$ (exptl) ^c
Carbon Tetrachloride					
MST	2.2	2.5	21.1	-1.8	-1.5
MC-FEP	2.4	2.8	20.7	-2.1	
Chloroform					
MST	1.8	1.2	20.9	-0.9	-0.8
MC-FEP	1.9	1.1	20.3	-0.8	
Aqueous Solution					
MST	-0.1	-3.3	20.1	2.0	$>0.7^d$
MC-FEP	0.7	-2.7	19.6	1.8	

^a Determined from addition of MST or MC-FEP differences in the free energy of solvation to the relative free energies in the gas phase. ^b $K = [\text{tetrazole}]/[\text{azido}]$. ^c Reference 12a. ^d The experimental value of 0.7 corresponds to the equilibrium constant in hexametapol solution. In a more polar solvent, the equilibrium constant is expected to be greater than this value (see ref 12a,c).

the reaction rate in solution. There is no experimental data directly available for comparison, but the activation energies for related reactions are quite close. Thus, the free energy barrier for the ring opening of 1-(*p*-chlorophenyl)pentazole in $\text{CD}_3\text{OD}-\text{CD}_2\text{Cl}_2$ is estimated to be 19.2 kcal/mol in the range of temperature from -10 to 0 °C,⁴² and the activation energy for cyclization of guanyl azide and its nitro derivative ranges from 18 to 21 kcal/mol in water,^{9b} which compares with our results. Even though direct comparison is not feasible, our estimate of the free energy barrier seems reasonable in light of the available experimental information.

The *trans*-azido is less stable than the *cis*-azido in carbon tetrachloride and chloroform, but their stabilities are similar in water. The change in the relative population of the two azido forms as the solvent's polarity is enlarged may influence the cyclization reaction, since the attack of the lone pair on N3 to the azido group requires a syn orientation,⁴³ and this stereo-electronic requirement is only fulfilled in the *cis*-azido isomer. To examine this point, the transition state for the conversion between *cis*- and *trans*-azido was localized at the MP2/6-311G(d) level. In this structure, the azido group lies perpendicular to the thiazole ring and the energy difference at the QCISD(T)/6-311++G(d,p) level with regard to the *cis*-azido species is only 5.1 kcal/mol, which agrees with the small degree of conjugation in the bond C2-N6 (see Table 3).⁴⁴ This torsional barrier is sensibly smaller than the relative energy of the transition state for the isomerization reaction (see Table 2), and accordingly, it seems that the *cis*-*trans* conformational equilibrium should have little influence on the isomerization process.

Effect of Substituents. The role of substituents was examined considering the 4-methyl, 5-methyl, and 5-chloro derivatives of thiazole[3,2-*d*]tetrazole, which were chosen owing to the availability of experimental equilibrium constants. To analyze the effect of substituents, a computational strategy that combines high-level ab initio calculations for a molecular subsystem with low-level calculations for the other subsystem

(42) Butler, R. N.; Collier, S.; Fleming, A. F. M. *J. Chem. Soc., Perkin Trans. 2* **1996**, 801.

(43) (a) Hegarty, A. F.; Mullane, M. *J. Chem. Soc., Chem. Commun.* **1984**, 913. (b) Hegarty, A. F.; Brady, K.; Mullane, M. *J. Chem. Soc., Perkin Trans. 2* **1980**, 535. (c) Zecchi, G. *Synlett* **1992**, 858.

(44) For comparison purposes, the values for the critical points of the C-C bonds in ethane and ethylene at the HF/6-31G(d) level are 0.252 and 0.363. See: Gatti, C.; MacDougall, P. J.; Bader, R. F. W. *J. Chem. Phys.* **1988**, *88*, 3792.

Table 6. Relative Gas-Phase Energies and Free Energies (kcal/mol) of *trans*-Azido and Tetrazole Species with Regard to the *cis*-Azido Isomer for 4-Methyl, 5-Methyl and 5-Chloro Derivatives

compd	<i>trans</i> -azido	tetrazole
Relative Energy (MP2/6-31G(d)) ^a		
4-methyl	2.4	2.4
5-methyl	2.3	3.2
5-chloro	2.5	5.2
Relative Energy (Composite) ^b		
parent compd	2.6	1.2
4-methyl	2.6	-0.8
5-methyl	2.5	0.0
5-chloro	2.7	2.0
Relative Free Energy (Composite)		
parent compd	2.3	3.5
4-methyl	2.3	1.5
5-methyl	2.2	2.3
5-chloro	2.4	4.3

^a Values determined from MP2/6-31G(d) geometry optimizations.^b Determined upon addition of the energy differences for the substituted compound to the best estimate of relative energies for the parent compound (see Table 2).

was adopted.⁴⁵ Particularly, the molecular geometry was optimized at the MP2/6-31G(d) level, and the corresponding energy differences between azido and tetrazole species for the substituted compounds with regard to the values determined for the parent compound at this level of theory were added to our best estimate of the gas-phase relative energies given in Table 2. From the composite values of the gas-phase energy differences, the free energy differences between isomers of the substituted compounds were estimated. Finally, the free energies of solvation of the derivatives were determined from SCRF-MST calculations, and they were used to estimate the relative stabilities in solution.

Table 6 reports the results in the gas phase. Attachment of methyl or chloro groups does not alter the energy difference between azido conformers, but they greatly change the relative energy of the tetrazole species. Thus, with regard to the parent compound, methylation stabilizes the tetrazole form by 1.2–2.0 kcal/mol, whereas the chloro substituent destabilizes the cyclized form by 0.8 kcal/mol. From the estimated differences in free energy, the population of tetrazole (around 8% for the 4-methyl derivative) increases by 1 order of magnitude with regard to the parent compound, whereas a 5-fold decrease is predicted for the population of the chloro derivative. These results can be realized from the influence on the electron delocalization in the tetrazole ring, which compensates or enhances the deactivating effect of the pyridine-type nitrogens depending on the nature of the substituent. Such an effect has also been examined in the shift of the equilibrium to the tetrazole form in the case of azapentalene anions.^{39,46}

The differences in free energy of solvation of *trans*-azido and tetrazole with regard to the *cis*-azido isomer are given in Table 7. Methylation does not modify significantly the solvation of both azido and tetrazole species. The chloro group has also negligible influence on the relative free energy of solvation of *trans*-azido, but its effect on the solvation of tetrazole is more

Table 7. Relative Free Energies of Solvation (kcal/mol) of *trans*-Azido and Tetrazole Species in Carbon Tetrachloride, Chloroform, and Aqueous Solution Determined from SCRF-MST Calculations for 4-Methyl, 5-Methyl, and 5-Chloro Derivatives^a

compd	<i>trans</i> -azido	tetrazole
Carbon Tetrachloride		
parent compd	-0.1	-1.0
4-methyl	-0.2	-0.9
5-methyl	-0.2	-1.0
5-chloro	-0.1	-0.6
Chloroform		
parent compd	-0.5	-2.3
4-methyl	-0.6	-2.1
5-methyl	-0.6	-2.4
5-chloro	-0.5	-1.7
Aqueous Solution		
parent compd	-2.4	-6.8
4-methyl	-2.2	-6.4
5-methyl	-2.3	-6.8
5-chloro	-2.2	-6.0

^a Values are given relative to the free energy of solvation of the *cis*-azido isomer. The MP2/6-31G(d) gas-phase optimized geometry was used in calculations.**Table 8.** Free Energy Differences (kcal/mol) in Solution of *trans*-Azido and Tetrazole Species with Regard to the *cis*-Azido Isomer for 4-Methyl, 5-Methyl, and 5-Chloro Derivatives^{a,b}

compd	<i>trans</i> -azido	tetrazole	log <i>K</i> (calcd)	log <i>K</i> (exp) ^c
Carbon Tetrachloride				
parent compd	2.2	2.5	-1.8	-1.5
4-methyl	2.1	0.6	-0.5	-0.7
5-methyl	2.0	1.3	-0.9	NA ^d
5-chloro	2.3	3.7	-2.7	NA
Chloroform				
parent compd	1.8	1.2	-0.9	-0.8
4-methyl	1.7	-0.6	0.4	0.1
5-methyl	1.6	-0.1	0.0	0.2
5-chloro	1.9	2.6	-1.9	<-1.3
Aqueous Solution ^e				
parent compd	-0.1	-3.3	2.0	>0.7
4-methyl	0.1	-4.9	3.3	>1.5
5-methyl	-0.1	-4.5	3.0	>1.3
5-chloro	0.2	-1.7	1.0	>-0.2

^a The calculated and experimental equilibrium constants for the azidoazomethine–tetrazole isomerization are also given. ^b See footnotes to Table 5. ^c Reference 12a. ^d Not available. ^e Experimental value in hexametapol (parent compound) or dimethyl sulfoxide (methyl and chloro derivatives). In a more polar solvent, the equilibrium constant is expected to be greater than this value (see ref 12a,c).

important, especially as the solvent polarity increases. Thus, hydration of this latter isomer for the 5-chloro derivative is less favored than for the parent compound by near 1 kcal/mol.

The free energy differences in solution are given in Table 8. The results reveal the influence exerted by substituents, which mainly modulate the gas-phase relative stability (see above). Methylation enhances the stability of the tetrazole, which is the preferred form even in chloroform. The destabilization of tetrazole upon chlorination is also apparent, as noted in the decrease (around 50%) of the free energy difference between *cis*-azido and tetrazole for the 5-chloro derivative with regard to the parent compound in water. The changes in the relative stability lead to notable variations in the calculated equilibrium constants (see Table 8), which compare satisfactorily with the experimental values,⁴¹ as stated from inspection of Figure 4, where the calculated and experimental values of log *K* for the different derivatives and solvents are shown. Inspection of Figure 4 shows the great influence of both solvation and substituents on the azido–tetrazole equilibrium. Indeed, it is

(45) (a) Froese, R. D. J.; Humbel, S.; Svensson, M.; Morokuma, K. *J. Phys. Chem. A*, **1997**, *101*, 227. (b) Noland, M.; Coitiño, E. L.; Truhlar, D. G. *J. Phys. Chem. A* **1997**, *101*, 1193. (c) Curtiss, L. A.; Raghavachari, K.; Trucks, G. W.; Pople, J. A. *J. Chem. Phys.* **1991**, *94*, 7221. (d) Montgomery, J. A., Jr.; Ochterski, J. W.; Petersson, G. A. *J. Chem. Phys.* **1994**, *101*, 5900. (e) Field, M. J.; Bash, P. A.; Karplus, M. *J. Comput. Chem.*, **1990**, *11*, 700.(46) Cano Gorini, J. A.; Farras, J.; Feliz, M.; Olivella, S.; Solé, A.; Vilarrasa, J. *J. Chem. Soc., Chem. Commun.* **1986**, 959.

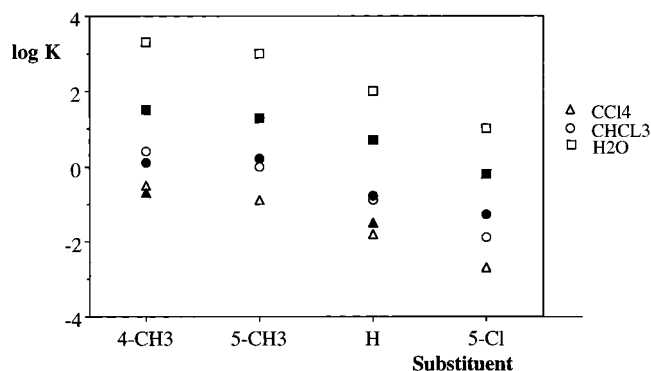


Figure 4. Representation of $\log K$ versus the substituent attached to the thiazole ring for carbon tetrachloride, chloroform, and aqueous solutions. White (black) symbols denote the theoretical (experimental) values. Note that the experimental values for aqueous solution are, in fact, lower bounds to the values of $\log K$, as they were determined in hexametapol (H) and dimethyl sulfoxide (4-Me, 5-Me, and 5-Cl). Note also that for the 5-chloro derivative the experimental value in chloroform is an upper bound.

also clear that the two effects are, at a large extent, separable, as noted by the parallel arrangement of the values for the different solvents.

Conclusions

High-level *ab initio* quantum mechanical calculations has allowed us to gain insight into the factors that modulate the azido–tetrazole isomerism of thiazole[3,2-*d*]tetrazole. The large electron density redistribution arising upon cyclization makes it necessary to use extended basis and to include high-order electron correlation terms to describe the gas-phase thermodynamics, which indicates clearly the gas-phase preference of the azido species. This means that the contribution due to the resonance energy in the tetrazole species does not compensate the destabilization arising from the deactivating effect of the pyridine-type nitrogens.

The analysis of the electron density in azido, tetrazole, and transition-state structures has revealed the complexity and asynchronism in the electron redistribution, which permits to differentiate different chemical events along the cyclization. The

reaction proceeds initially through loss of the linearity of the azido group, approaching the nitrogen N8 to the pyridine-type nitrogen N3 of the ring, and this step is then followed by the attack of the lone pair on N3 to the azido group, leading to formation of the bond between N3 and N8. The changes in electron density associated to these events give rise to a large free energy barrier in the gas phase.

The results clearly show the change in the relative stability between azido and tetrazole isomers as the polarity of the solvent is enlarged, which can be explained by the larger polarity of the tetrazole and by the larger solvent-induced polarization of this latter species. It is also worth noting the sensibility of the equilibrium to substituents. The results suggests that the substituent leads to notable changes in the intrinsic stability of azido and tetrazole isomers in the gas phase, the equilibrium being displaced toward the cyclized or open forms by electron-donating or electron-withdrawing substituents. Overall, the influence of both solvent polarity and substituents is found to be separable at a great extent. Therefore, this opens the way to control the stability of the tetrazole ring simply by choosing appropriately the contribution of these two factors. Undoubtedly, these findings can be valuable to design synthetic routes of tetrazole compounds.

Acknowledgment. We are indebted to Prof. J. Elguero for encouraging discussions. We are also indebted to Profs. M. Cossi and J. Tomasi for kindly providing us with a copy of the modified version of HONDO-8. We also thank Prof. R. F. W. Bader for making available the AIMPAC program. Finally, Prof. W. L. Jorgensen is acknowledged for a copy of BOSS3.4 computer program. This work was supported by the Centre de Supercomputació de Catalunya (C4; Molecular Recognition Project) and by the Dirección General de Investigación Científica y Técnica (DGICYT; Grants PB93-0779 and PB94-0940).

Supporting Information Available: Optimized geometries at the HF and MP2 levels with different basis sets for azido, tetrazole, and transition-state structures and locations of bond critical points (6 pages, print/PDF). See any current masthead page for ordering information and Web access instructions.

JA9726724